

Research Article

A Cyborg Insect Reveals a Function of a Muscle in Free Flight

T. Thang Vo-Doan ^{1,2}, V. Than Dung,¹ and Hirotaka Sato ¹

¹Nanyang Technological University, School of Mechanical and Aerospace Engineering, Singapore

²University of Freiburg, Institute of Biology I, Germany

Correspondence should be addressed to Hirotaka Sato; hirosato@ntu.edu.sg

Received 18 January 2022; Accepted 21 March 2022; Published 4 May 2022

Copyright © 2022 T. Thang Vo-Doan et al. Exclusive Licensee Beijing Institute of Technology Press. Distributed under a Creative Commons Attribution License (CC BY 4.0).

While engineers put lots of effort, resources, and time in building insect scale micro aerial vehicles (MAVs) that fly like insects, insects themselves are the real masters of flight. What if we would use living insect as platform for MAV instead? Here, we reported a flight control via electrical stimulation of a flight muscle of an insect-computer hybrid robot, which is the interface of a mountable wireless backpack controller and a living beetle. The beetle uses indirect flight muscles to drive wing flapping and three major direct flight muscles (basalar, subalar, and third axillary (3Ax) muscles) to control the kinematics of the wings for flight maneuver. While turning control was already achieved by stimulating basalar and 3Ax muscles, electrical stimulation of subalar muscles resulted in braking and elevation control in flight. We also demonstrated around 20 degrees of contralateral yaw and roll by stimulating individual subalar muscle. Stimulating both subalar muscles lead to an increase of 20 degrees in pitch and decelerate the flight by 1.5 m/s^2 as well as an induce in elevation of 2 m/s^2 .

1. Introduction

Developing insect-inspired flapping wing micro aerial vehicles (MAVs) has drawn lots of interest from engineers in the recent decades due to the higher efficiency of insect flight as compared to traditional rotational wings [1–16]. Although great efforts and resources were expended to optimize the structural and material design of the MAVs toward untethered autonomous and endurance flight, it is still challenging to match the performance capability of the insects in terms of actuating, sensing, energy efficiency, and locomotion control. While the centimeter-scale flyers used a combination of small electromagnetic motors, linkages, and crank or pulley-string to drive the wings [4–6, 15], the millimeter-scale ones required piezoelectric actuators or soft dielectric elastomer actuators and compliant mechanisms to generate wing flapping [2, 4, 7, 8]. Tilting the whole flapping mechanism to alter stroke plane [4, 5] and generating passive wing rotation or asymmetric flapping frequencies and amplitudes [2, 4, 7, 9] were also implemented to control the flight of MAVs. Simplifying flight mechanisms due to size and weight limit makes MAVs not able to match the agile flight control of the insects as the native flyers can control wing kinematics both passively and actively by activating indirect and direct flight muscles [4, 17]. Scaling the robots to insect

size also faces a bottle neck in durability of materials (e.g., actuators and chassis) that limit their life cycle significantly [2, 4, 5, 7, 9, 16]. Furthermore, free flight endurance is still a challenge as the current longest flight of flapping MAVs is less than 12 min due to high power consumption of the actuators along with wireless communication and sensors. While it took engineers years or even decades to achieve a perfect insect-scale MAV [1–16], insects are already perfect flyers. They consist of indirect flight muscles for flapping the wings, direct flight muscles for altering wing kinematics, and resilient cuticle of thorax and wing hinges that can last for a lifetime. They also have a complex sensory and neural network for precise feedback control of motor actions. Insects have more agile maneuverability in flight as they can control wing kinematics both actively and passively to easily turn, adjust altitude, body angles, hover, and even have extreme motion like saccade [18–24]. Thus, MAV based on living insect platform would be a preferred model that inherits the insect's high efficiency, maneuverability, and endurance in flight while bypassing complex mechanical and material design, fabrication process, and high power consumption issue [25–29].

The interface of a living insect platform and a mounted control backpack results in a resilient insect-computer hybrid robot, also known as cyborg insect, or insect biobot.

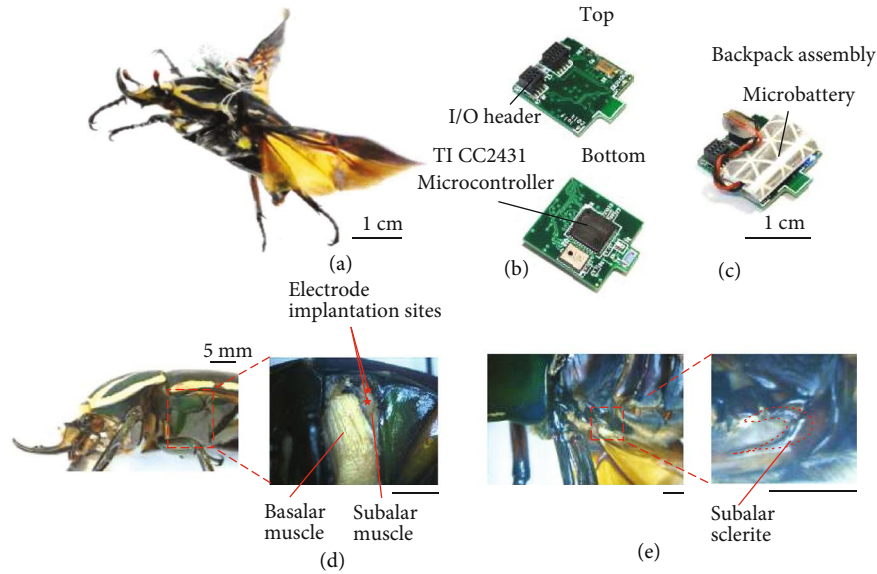


FIGURE 1: Overview of an insect-computer hybrid robot. (a) Live beetle with mounted backpack. (b) The wireless backpack (electrical stimulator) was customized using the TI CC2431 microcontroller with the tiny I/O header for connecting the electrodes and a microbattery. (c) The battery was wrapped with retro-reflective tape and mounted on the top of the backpack to supply power and serve as a marker for motion tracking. (d) Lateral view of the beetle with a close-up view of the direct flight muscles after dissecting the cuticle. The subalar muscle is located in the posterior part of the thorax, next to the basalar muscle. It runs from the hind leg coxa to an apodema that connects to the subalar sclerite. (e) Dorsal view of the beetle after removal of the elytra. Exposed view of the subalar sclerite showing connection to the wing base via a flexible membrane.

The motor actions of the insect can be controlled by sending the electrical stimulus directly from the backpack terminals to the muscles or neural clusters through implanted electrodes. Precise walking gaits in beetles were achieved by stimulating the leg muscles [30, 31] while turning, backward, forward, and sideways walking were driven by stimulating the mechanosensory organs (e.g., antennae, cercus, and elytra) and ganglion in beetles [32, 33] and cockroaches [34–36]. Flight initiation and cessation of the beetles were achieved by stimulating optic lobes [27] and indirect flight muscles [37] while stimulating direct flight muscles enable steering control in flight [25, 27, 28]. In addition, there were also attempts to control moth flight by direct stimulation of insect brain areas [38], ventral nerve cord that controls abdominal deflection [39], and antennal muscles [29]. Although various insect platforms were evaluated for MAV application, giant flower beetles were superior candidates due to not only their agile flight capability but also their firm exoskeleton to protect themselves from crashes and high payload to carry heavy backpack and battery [25–27, 29, 40]. While stimulating basalar muscles (Figure 1) increase the wing beat amplitude that cause contralateral turn [27], the activation of third axillary muscle (3Ax) resulted in ipsilateral turn due to decrease in wing amplitude in beetles [25]. In addition, stimulating basalar and 3Ax muscle alternatively with a feedback control system could drive the beetle to follow a predetermined path or altitude in flight [28, 41]. Although tuning wing amplitudes for turning control of beetle flight is well established, the control of wing rota-

tion for body angles and braking is lacking. Such capability of body angle and braking control would enable more complex maneuverability of beetle flight such as hovering, perching, and saccade.

Here, we demonstrated a stimulation protocol of subalar muscle, the last major direct flight muscle besides basalar and 3Ax muscles, to control the braking and body angles of an insect-computer hybrid robot based on a live beetle (*Mecynorrhina torquata*) in flight (Figures 1(a)–1(c)). During fictive decelerated flight in tethered condition, the firing rate of subalar muscle and the wing rotation angle increased which suggested the role of subalar muscle in braking and pitch control. Stimulating individual subalar muscle in free flight induced contralateral yaw and roll of the body as well as increase in pitch angles. Moreover, stimulating both subalar muscles simultaneously also resulted in braking and elevation in flight.

2. Materials and Methods

2.1. Animal. Adult *Mecynorrhina torquata* beetles (6 cm–8 cm, 8–10 g) were imported from Kingdom of Beetle, Taiwan, and reared in separate containers (20 × 8 × 12 cm) with woodpile bedding. They were fed sugar jelly every 3 days. The temperature and humidity of the rearing room were maintained at 25°C and 60%. Invertebrates, including beetles, does not require ethics approval for animal research according to the National Advisory Committee for Laboratory Animal Research.

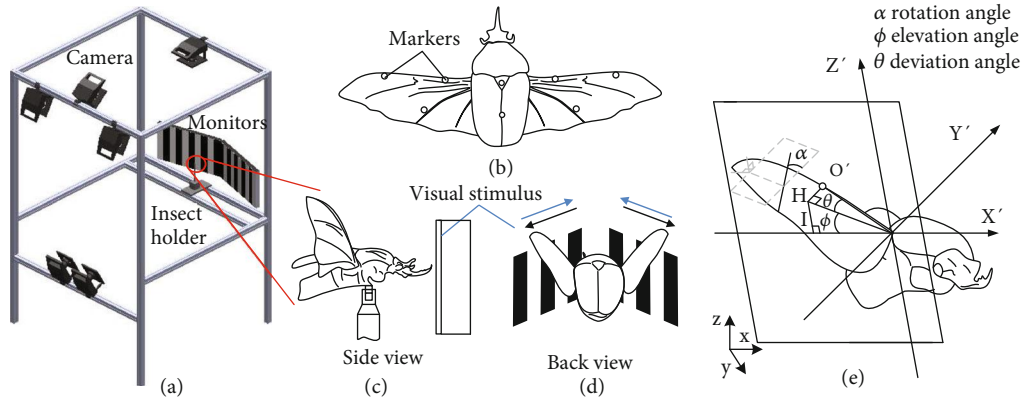


FIGURE 2: Tethered experiment setup. (a) Six near-infrared cameras were mounted onto an aluminum frame to cover a volume of $400 \times 400 \times 400$ mm surrounding the beetle holder at a frame rate of 1500 fps. The beetle was fixed on the holder with the head towards the two monitors (placed at 250 mm from the beetle head) to see the moving pattern generated. For visual stimulation, the patterns were 20 mm black/white horizontal stripes moving forward and backward at 50 Hz within the screen. During electrical stimulation, the moving stripes were changed to a still white background on the screen. (b) Each wing was attached to three retro-reflective tape markers (2×2 mm) for reconstructing the wing kinematics and two markers on the body for reference. (c, d) Lateral and posterior view of the tethered beetle presented visual stimulus of vertical stripes from the panel. (e) The wing position was defined with a 60° tilted body axis after rotating the wing stroke plane (SP) to the horizontal plane for calculation. The three Euler angles of the wing (ϕ , elevation; θ , deviation; and α , wing rotation angles) were defined. The elevation angle is the wing stroke angle measured about the Y' axis in the mean stroke plane, the deviation angle is the out-of-plane angle that the leading edge of the wing makes with the stroke plane, the wing rotation angle is the angle the wing cord makes with the plane created by the leading edge and the Y' axis, and $(X' Y' Z')$ is the wing stroke plane frame.

2.2. Electrode Implantation. Beetles were anesthetized for 3 min in a small CO_2 -filled container. The beetle was then placed on a wooden block and gently covered with dental wax, which was presoftened by dipping into hot water. Two silver wire electrodes (diameter of the bare wire, $127 \mu\text{m}$, and diameter of the coated wire, $178 \mu\text{m}$; A-M Systems) were implanted into the subalar muscle at a depth of 3 mm through a small opening on the cuticle. Before the electrodes were inserted, the bare silver was exposed by flaming. The electrodes were secured in place by melted beeswax.

2.3. Wireless Backpack Assembly. The wireless system included two electronic devices that were based on the TI CC2431 microcontroller [25]. One was the miniature wireless backpack, which was mounted onto the beetle, and the other was the base station connected to the computer. The backpack was driven by a micro poly lithium-ion battery (Fullriver, 3.7 V, 350 mg, 10 mAh) wrapped with retro-reflective tape (Silver-White, Reflexite), which also served as a marker for the motion capture system. The total mass of the backpack, including the battery, was 1.2 ± 0.26 g. The additional mass from the backpack has minimal effect on beetle flight speed. The backpack mounted beetles behaved as close as load-free beetle while excessive load significantly decreased the velocity of the beetle flight (Figure 1 and S1).

An IMU backpack was used to record the body angles and accelerations of the flying insect. The backpack contains a nine axis IMU MPU9250 from InvenSense to measure orientation and movement of the board and the BLE microcontroller CC2642R from Texas Instrument. The IMU integrates a small digital computational engine to do sensor fusion from its nine axes of data sensor which 3-axis acceler-

ation, 3-axis gyroscope, and 3-axis magnetometer. The IMU sensor results in three linear accelerations and the sensor orientations in quaternion format. The IMU was sampled with sampling rate 100 Hz. The total mass of the backpack, including the battery, was 1.6 ± 0.26 g.

2.4. Tethered Experiment. The beetle was placed within the field of view of six near-infrared cameras (VICON T40s) in the three-dimensional (3D) motion capture system (Figure 2(a)) to record wing kinematics. Retro-reflective markers were attached to the wings and body of the beetle (Figure 2(b)); then, the silver wire electrodes were implanted into the subalar muscle and connected to the EMG recorder (CC2431 Microcontroller Development board) through an instrument amplifier (Analog Devices, LT1920) or a function generator. For visual stimulation, a visual stimulator was set to project the optic flow pattern (vertical black/white stripes of 20 mm) onto two monitors placed 250 mm in front of the beetle (Figures 2(c) and 2(d)). When the patterns moved, the beetle changed the wing kinematics to track the moving patterns. The EMG signal was recorded from the subalar muscle and synchronized with the wing kinematics (Figure 2(e)). For electrical stimulation, the wing kinematics were synchronized with the electrical stimulus. Change in wing stroke plane is not considered as activating subalar muscle does not alter wing stroke plane [41].

2.5. Free Flight Experiment. The experiment was conducted in a flight arena of $12 \times 8 \times 4$ m covered by a motion capture system equipped with 20 near-infrared cameras (VICON, T40s, and T160). After assembly, the wireless connection to the backpack and operation laptop was set

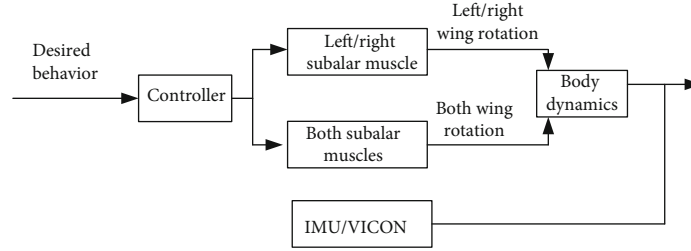


FIGURE 3: Block diagram of free flight experiment. To change individual left/right wing rotation, left/right subalar muscle was stimulated. Stimulating both subalar muscles to change rotation angle of both wings simultaneously. The body dynamics of the beetle were then obtained by IMU on the backpack or the motion capture system.

up. The beetle was then released into the flight arena and stimulated via a Wii remote. Activation of the Wii remote sent a command to the BeetleCommander running on the laptop, which sent a wireless command to the backpack via the base station. After receiving the command, the backpack generated the electrical stimulus signal and applied it to the subalar muscle. The beetle position was recorded simultaneously by the 3D motion capture system or the IMU data is then synchronized with the electrical stimulation. The work flow of free flight stimulation experiment is shown in Figure 3.

A 500 ms pulse train was applied on the subalar muscle in free flight for electrical stimulation. The pulse amplitude and pulse width are 3 V and 3 ms, respectively (Figure S2). The stimulation frequency is varied from 40 Hz to 100 Hz. The stimulation parameters were selected from a brief survey at the beginning of the experiment setup and limited to the most effective range due to the constrain of flight duration of the beetles. Besides, the electrical stimulation of subalar muscle does not affect other nearby muscles (Figure S3).

The free flight trajectories of the beetles were sorted to individual flight paths of 150 ms before stimulation and 500 ms during stimulation. The x , y , and z components of the velocity and acceleration were calculated after smoothing the flight path using a 5th order polynomial function by a customized MATLAB code ($N_{\text{both}} = 14$ beetles, $n_{\text{both}} = 495$ trials, $n_{\text{left}} = 360$ trials, $n_{\text{right}} = 346$ trials). Saccade flight paths whose angular velocities were over $500^\circ/s$ were excluded from the data analysis because such a fast motion could not be accurately detected. The horizontal and lateral vectors were calculated for every pair of points along the flight path on the (x, y) plane. The horizontal and lateral accelerations were calculated by summing the projected x and y accelerations relative to the horizontal and normal vectors, respectively. The vertical acceleration is the z component of the acceleration.

The IMU data was collected from different beetles ($N = 10$ beetles, $n_{\text{both}} = 573$ trials, $n_{\text{left}} = 277$ trials, $n_{\text{right}} = 207$ trials). A 5th order Butterworth filter with cutoff frequency of 20 Hz was applied for acceleration data. The induced amount is defined as the difference of the peak value within first 300 ms during stimulation and the onset value.

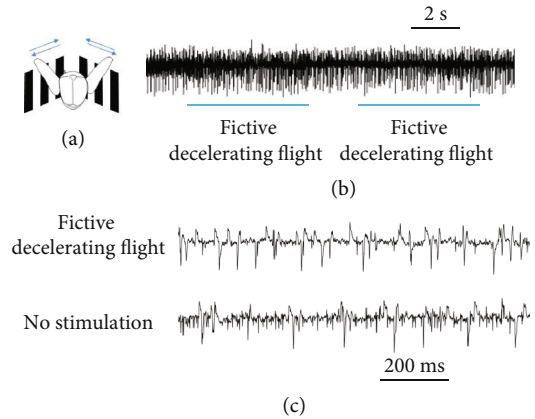


FIGURE 4: Electromyography of the beetle during visual stimulation. (a) The beetle was mounted in front of two monitors (form an angle of 120 degrees) for visual stimulation. Vertical black/white stripes moved at around 10 Hz to emulate forward/backward visual stream. A pair of silver electrodes were implanted into the subalar muscle for recording EMG signal. (b) The subalar muscle fired continuously during beetle flight. (c) It was most active during fictive decelerating flight, with a firing rate of 25.3 Hz, which decreased to 21.6 ($p < 0.05$, paired sample t -test) during the period of no stimulation.

2.6. Statistical Analysis. The paired sample t -test was performed to check the significance of the beetle responses before and during stimulation. The one simple t -test was used to check if the induced acceleration or angle was significant. Spearman correlation test was used to check the significance of the graded responses. A p value less than 0.05 was considered statistically significant.

3. Results

3.1. The Role of Subalar Muscle. The beetle subalar muscle is inserted from the hind leg coxa to the apodema of the subalar sclerite [20, 24]. The subalar muscle lies next to the basalar muscle at the posterior end of the thorax (Figures 1(d) and 1(e)). Its function would be similar to those of the III1 muscle of the blowfly [41, 42], M99 and M129 muscles of the locusts [26, 43–45] due to similarity in configuration. Anatomically, the contraction of the subalar muscle pulls

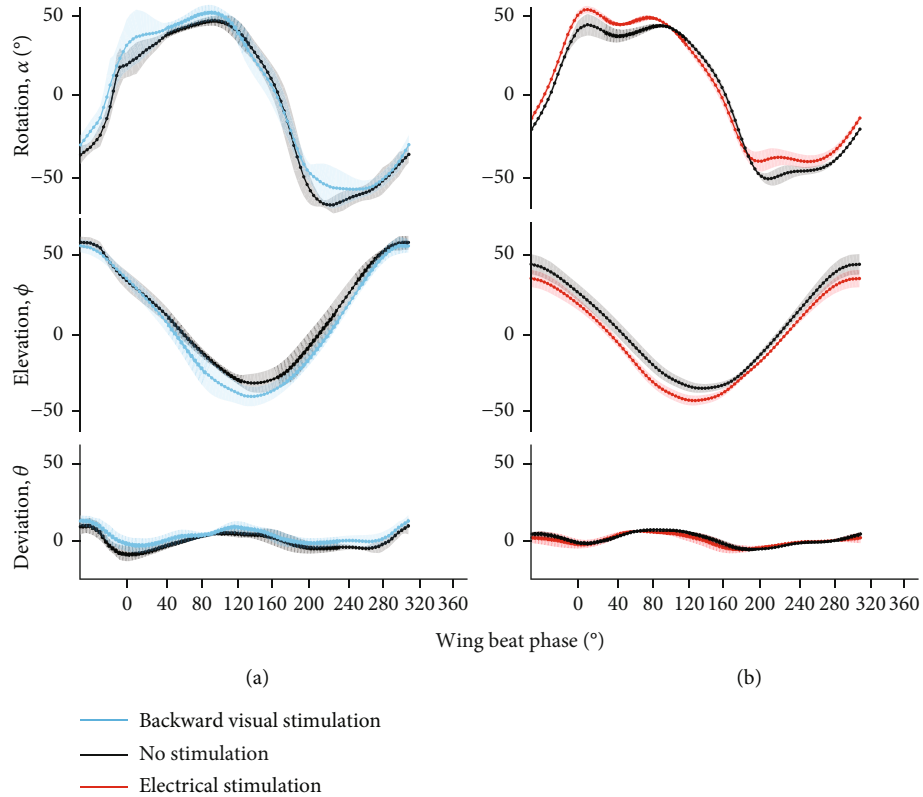


FIGURE 5: Wing beat trajectories recorded during visually stimulated fictive decelerating flights ($N = 4$, $n = 20$ trials) and electrical stimulation of subalar muscle ($N = 4$, $n = 98$ trials). (a) The backward visual stimulation induced a positive phase shift with a 10° increase ($p < 0.05$, paired sample t -test) in the wing rotation angle from 80° to 180° and from 220° to 300° of the wing cycle. No change was observed in the deviation angle ($p > 0.05$, paired sample t -test) while the wing elevation angle showed a reduction of 10° from 80° to 180° of the wing cycle. The insert represents the magnification of the wing rotation angle at the phase with the highest change. (b) The beetle showed a slight phase shift during the first 80° of the wing cycle and a clear increase of 10° ($p < 0.05$, paired sample t -test) in wing rotation from 80° to 180° and from 220° to 300° of the wing cycle when the subalar muscle was stimulated. No change was observed in wing deviation angle while there is a negative shift of 10° in wing elevation angle.

the posterior part of the wing base, consequently, and depresses the trailing edge of the wing that increases the wing rotation angle and thus the wing angle of attack. This would lead to a decrease in thrust and increase in lift generated by the wings of the flying insect [42–45]. Such change in thrust and lift of the wings would alter the body angles or induce brake in flight [21, 42–46].

The beetle subalar muscle was innervated in a graded fashion under tethered condition. It was more active during fictive decelerating flight than nonstimulated flight (Section 2.4). During flight, we observed that the subalar muscle was continuously active (Figure 4(a)). We provided optic flow stimuli to induce fictive decelerating flight in tethered beetles [23, 45, 47]. The firing rate of the electromyogram (EMG) spike during fictive decelerating flight was higher than that during no stimulation (Figure 4(b)) ($p < 0.05$, paired sample t -test). This would suggest that the beetle increases the activity of subalar muscle during braking in flight.

Whether stimulated due to fictive backward visual stimuli (Figure 5(a)) or via direct electrical stimulation (Figure 5(b)), enhanced activity in the subalar muscle caused increase

in wing rotation angle. Compared to spontaneous flight (black traces, Figure 5(a)), the wing rotation and elevation angles, respectively, increased during fictive decelerating flight, with only slight changes in the corresponding deviation angle ($N = 4$, $n = 20$, $p < 0.05$, paired sample t -test). Similar to braking in flight, electrical stimulation of subalar muscle led to the increment in wing rotation and elevation angles (Figure 5(b)) while little change was observed in the deviation angles ($N = 4$, $n = 98$, $p < 0.05$, paired sample t -test). These results would suggest that the beetle activates subalar muscle to increase wing rotation angle when braking in flight.

3.2. Body Angles Control of the Insect-Computer Hybrid Robot in Free Flight. In free flight, the beetle with mounted IMU backpack enabled us to record body angles and accelerations of the insect during flight (Figures 6(a)–6(c)). Stimulating either left or right subalar muscle also results in increase in pitch angle from 5 degrees to 22 degrees with a weak correlation with stimulation frequency (coefficient = 0.25, $p < 0.0001$, Spearman correlation test; linear regression: $\Delta\text{pitch}_i = 0.15 \times \text{Frequency} + 0.52$, $R = 20\%$)

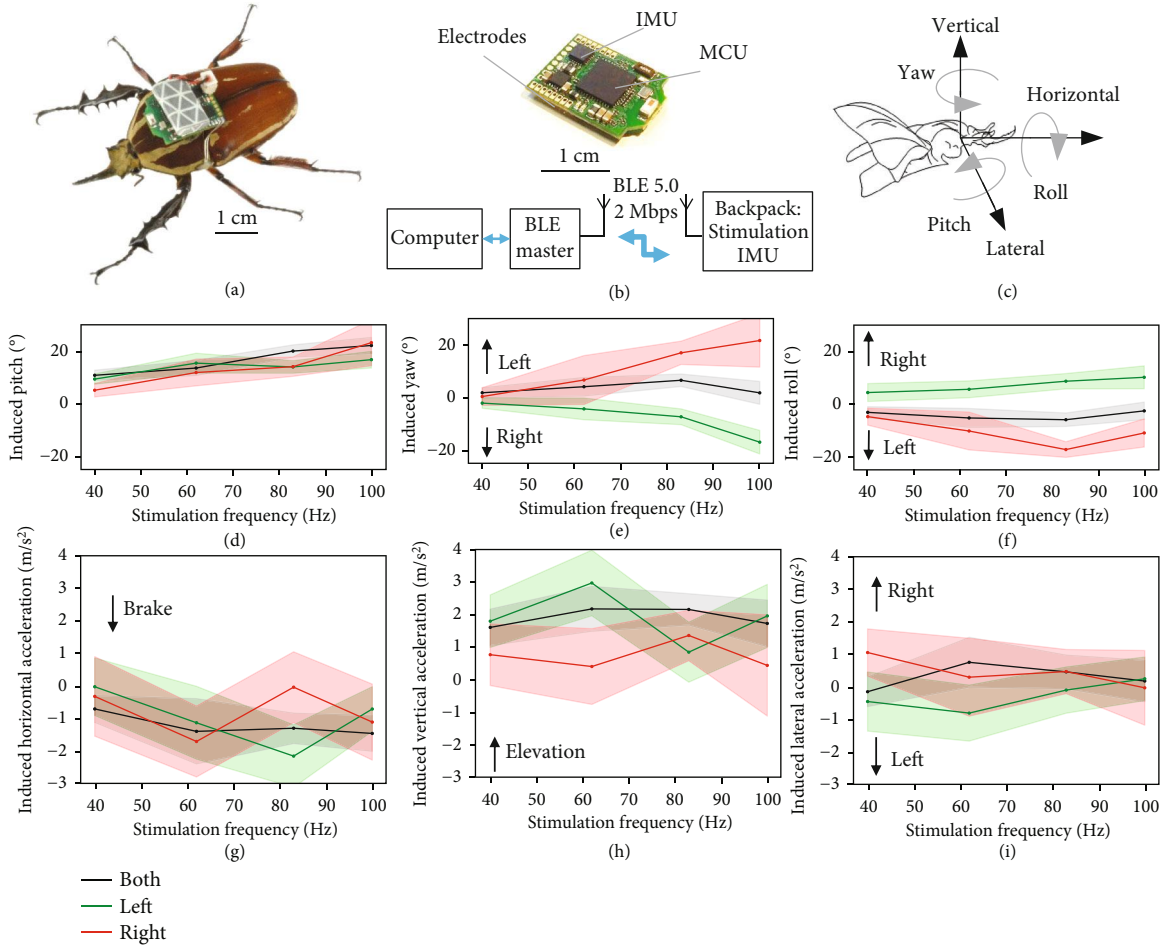


FIGURE 6: Remote electrical stimulation with IMU backpack during free flight ($N = 10$ beetles, $n_{\text{both}} = 573$ trials, $n_{\text{left}} = 277$ trials, $n_{\text{right}} = 207$ trials). (a) The IMU backpack mounted on the beetle. (b) The backpack consists of a Bluetooth low energy (BLE) CC2642R microcontroller and a nine-axis inertial measurement unit (IMU) MPU9250 from InvenSense. The backpack processes the commands from control program to execute control signals, collect, and return data. A computer communicates with the backpack via BLE 5.0 interface to transfer all control signal and collect and store all backpack information including stimulation signal and IMU data. (c) The positive direction of the accelerations and body angles. (d) The induced pitch angle of the beetle increased in all cases and graded by stimulation frequency. (e) The induced yaw angle increased contralaterally when stimulating individual subalar muscle. (f) The induced roll angle increased contralaterally when stimulating individual subalar muscle. (g) The horizontal acceleration of the beetle was decreased in all cases and was graded by increasing the stimulation frequency when both muscles were stimulated. There is no correlation of the horizontal acceleration and the stimulation frequency when individual muscle was stimulated. (h) The induced vertical acceleration remained positive when stimulating both subalar muscles. (i) There is slight ipsilateral increase in lateral acceleration when individual subalar muscle was stimulated. Black, green, and red lines represent the results of electrical stimulation of both, left, and right subalar muscles, respectively. Shaded regions indicate 95% confidence interval.

(Figure 6(d)). The increase in pitch angle was from 10 degrees to 22 degrees (coefficient = 0.23, $p = 0.013$, Spearman correlation test) and fitted by a linear regression ($\Delta\text{pitch}_{\text{both}} = 0.2 \times \text{Frequency} + 2.58$, $R = 28.28\%$) when both subalar muscles were stimulated while there is slight change in yaw and roll angles. Such increase in pitch angle would be the result of the induced lift of the wing during the stimulation which is similar to that found in *Drosophila* [43, 45, 48]. Stimulating individual subalar muscle led to graded contralateral increase in yaw angle from 2 degrees to 17 degrees (coefficient = 0.26, $p = 0.00017$, Spearman correlation test; linear regression: $\Delta\text{yaw}_i = 0.33 \times \text{Frequency} -$

8.75 , $R = 33.16\%$) and roll angle from 5 degrees to 10 degrees (coefficient = 0.19, $p = 0.0049$, Spearman correlation test; linear regression: $\Delta\text{roll}_i = -0.13 \times \text{Frequency} - 0.86$, $R = 20.16\%$) when the stimulation frequency was tuned from 63 Hz to 100 Hz (Figures 6(e) and 6(f)). The change in body yaw and roll angles would be due to the asymmetry of the wing rotation angles during the stimulation. The electrical stimulation of subalar muscle would increase the wing rotation angle that lead to the increase in lift of that side [44]. Such increases are associated with the increase in vertical acceleration and decrease in horizontal acceleration of the beetle during flight.

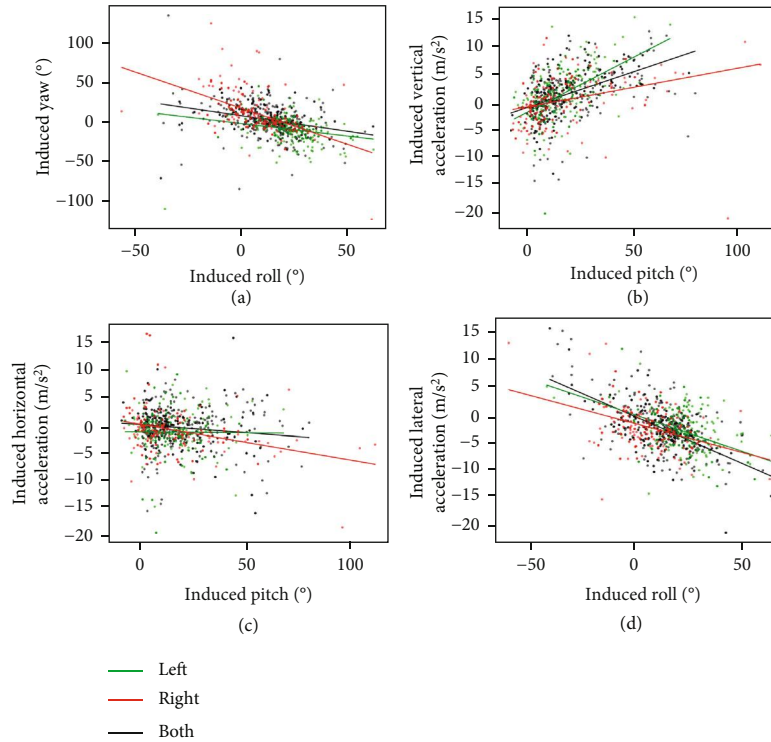


FIGURE 7: The correlation of induced accelerations and body angles. (a) The induced yaw and roll angles have a moderate correlation coefficient of -0.41 ($p < 0.0001$, Spearman correlation test). (b) The induced horizontal acceleration has a weak correlation coefficient of -0.13 with the induced pitch angle ($p = 0.0013$, Spearman correlation test). (c) The induced lateral acceleration has a weak correlation coefficient of -0.29 with the induced roll angle ($p < 0.0001$, Spearman correlation test). (d) The induced vertical acceleration has a moderate correlation coefficient of 0.49 with the induced pitch angle ($p < 0.0001$, Spearman correlation test).

3.3. Braking Control of the Insect-Computer Hybrid Robot in Free Flight. A decrease of 0.7 m/s^2 to 1.4 m/s^2 of horizontal acceleration (Figure 6(g)) and increase of 1 m/s^2 to 1.6 m/s^2 of vertical acceleration (Figure 6(h)) were observed when stimulating both subalar muscles. The increase in induced lateral acceleration of 0.5 m/s^2 to 1 m/s^2 when individual subalar muscle was stimulated would be a side slip (Figure 6(i)). There is decrease in horizontal acceleration and increase in vertical acceleration when individual subalar muscle was stimulated but without a clear trend of change (Figures 6(g) and 6(h)). In addition, the induced yaw angle has a moderate negative correlation with the induced roll angle (coefficient = 0.49 , $p < 0.0001$, Spearman correlation test), which is similar to that of a bank turn observed in *Drosophila* [15, 21] (Figure 7(a)). The increase in pitch angle is associated with the elevation during flight (correlation = 0.49 , $p < 0.0001$, Spearman correlation test) (Figure 7(b)). The induced horizontal acceleration and lateral acceleration have a weak correlation coefficient of -0.13 and -0.29 with the induced pitch and induced roll, respectively ($p = 0.0013$, Spearman correlation test) (Figures 7(c) and 7(d)). These correlations are also in agreement with those observed in *Drosophila* [43, 45]. These findings support our hypothesis that the subalar muscles have a function of controlling brake, elevation, and body angles of the beetles during free flight.

In addition, recorded positions of freely flying beetles showed the same tendency observed with IMU backpack. The stimulation of the subalar muscles led to the decrease in horizontal acceleration and increase in vertical acceleration (Figures 8(a) and 8(b)). The induced acceleration was computed from the free flight path data (refer to “Free Flight data analysis” and [25]). During free flight, we also found that the induced horizontal acceleration was negative (Figure 8(b)) and gradually reduced to -1.6 m/s^2 with a moderate dependence on the stimulation frequency (correlation = -0.55 , $p < 0.0001$, Spearman correlation; linear regression: $\Delta a_{\text{both}} = -0.02 \times \text{Frequency} - 0.09$, $R = 72\%$). In addition, stimulation of the subalar muscle induced a relatively small but significant 0.5 m/s^2 to 1 m/s^2 increase in the induced vertical acceleration ($p < 0.05$, one sample *t*-test) (Figure 8(c)). Stimulate left or right subalar muscle caused an increase in induced lateral acceleration of about 0.8 m/s^2 to 1.5 m/s^2 ipsilaterally when the stimulation frequency is within 70 Hz to 100 Hz ($p < 0.05$, one sample *t*-test) (Figure 8(d)). The decrease in the horizontal directions and increase in the vertical directions of the induced accelerations indicate the increase in drag and lift of the wings.

Our data showed that the role of subalar muscle in beetle flight is different from that of basalar and 3Ax muscles. While the activation basalar and 3Ax muscles cause increment and reduction in wing beat amplitude, respectively

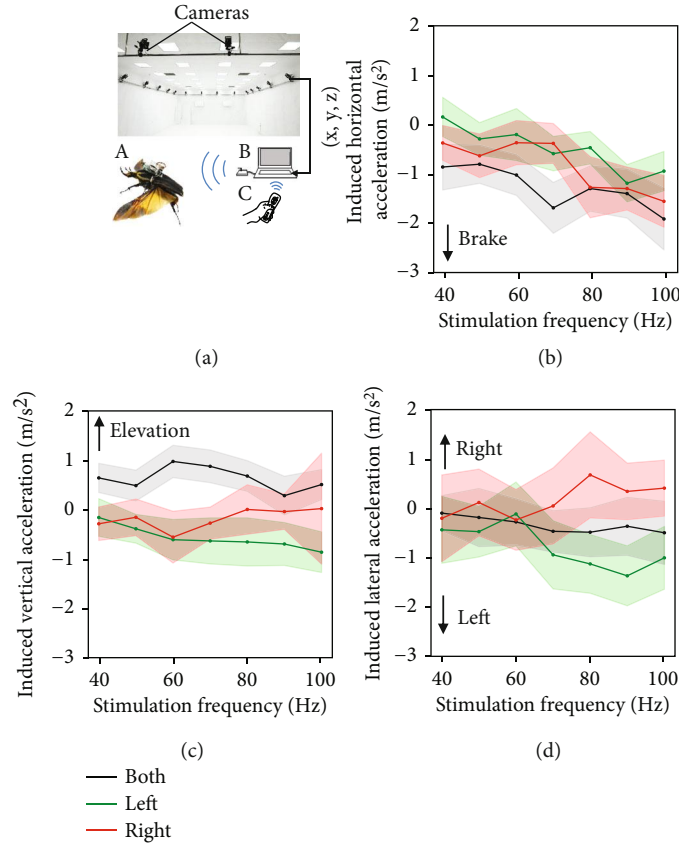


FIGURE 8: Remote electrical stimulation during free flight ($N_{\text{both}} = 14$ beetles, $n_{\text{both}} = 495$ trials, $n_{\text{left}} = 360$ trials, $n_{\text{right}} = 346$ trials). (a) The backpack (A) was mounted onto the beetle before releasing it into the air for free flight. The backpack wirelessly received the command from the operator's laptop via the base station (B) plugged into the laptop when the operator pressed the command button of the Wii remote (C). The backpack then applied the electrical stimulus to the subalar muscles. Meanwhile, the positions of the flying beetle were recorded with timestamps by the motion capture system (D) and fed into the laptop for synchronizing with the stimulation command. (b) The horizontal acceleration was graded by increasing the stimulation frequency. (c) The induced vertical acceleration remained positive when stimulating both subalar muscles while stimulating individual subalar muscles caused reduction in vertical acceleration. (d) The induced lateral acceleration shifted toward left when stimulating both subalar muscles. Stimulating individual muscle led to ipsilateral increment of induced lateral acceleration for the stimulation. The accelerations were calculated based on flight trajectories of the beetles. Shaded regions indicate 95% confidence interval.

[25, 27], activating subalar muscle leads to an increase in wing rotation angle. In addition, we found that activating subalar muscle in free flight induced change in body angles and braking which are distinct from the steering role of basalar and 3Ax muscles.

4. Discussion

Although there are graded responses of the pitch, yaw, roll, and horizontal acceleration of the beetle to electrical stimulation frequency, the low regression correlation is a potential issue for precise locomotion control with subalar muscle. Closing the control loop with feedbacks from IMU and motion capture data would improve the flight control. Despite of several attempts to implement feedback control for freely flying beetles, it is still a challenge to realize autonomous flight of insect-machine hybrid robot [28, 41]. It would be useful to have a detail physiology investigation on the role of individual flight muscles in control of wing

kinematics [49–51]. Such data would provide more insight of how the individual flight muscles work and their effect in flight and thus suggest appropriate stimulation protocol to control the flight muscles. For instance, the phasic activation pattern of a muscle would suggest the efficient stimulation timing of such muscle.

Recording activities of multiple muscles and high-resolution images of the wings in tethered condition is convenient and would provide certain relationship of muscle activation and wing kinematics [49, 50, 52, 53]. However, the behavior of insects in such constrained condition would differ from freely moving ones, and it is impossible to achieve complex behaviors of the insect such as hovering and perching in such condition. While a large-scale virtual reality system can help to reproduce complex behaviors of freely flying insect [54], free flight EMG recording of flight muscles [55–57] along with high-resolution recording of the wings and body [21, 58–60] would provide precise correlation of muscle activation patterns and flight maneuvers.

Implementing such data into a feedback control system would enable autonomous flight of insect-machine hybrid robots in the future.

Fully control the beetle flight requires the ability to activate multiple flight muscles. In this paper, we demonstrated that the role of subalar muscle in manipulating wing rotation angle which differs from regulating wing beat amplitude of basalar and 3Ax muscles. We were then able to control braking and lift as well as body angles of a beetle in free flight by activating subalar muscle. A feedback control system with the capability to stimulate all direct flight muscles would enable complex maneuver control of the beetle flight in the future.

Data Availability

All data needed to evaluate the conclusions in the paper are present in the paper or in the Supplementary Materials.

Conflicts of Interest

The authors declare no competing or financial interests.

Authors' Contributions

T.T.V.-D. and H.S. designed the research. V. T. D. designed the hardware and software for IMU backpack. T.T.V.-D. conducted the experiments, analyzed, and interpreted data. T.T.V.-D. and H.S. wrote the paper.

Acknowledgments

The authors would like to thank Mr. Duc Long Le, Mr. Huu Duoc Nguyen, and Dr. Li Yao for the discussion and Mr. Roger Tan Kay Chia, Mr. Chew Hock See, and Mr. Seet Thian Beng for their support. This work was partly supported by the Singapore Ministry of Education (RG140/20) and SPring-8 in Japan with the approval of the Japan Synchrotron Radiation Research Institute (Nos. 2015A1502, 2015B1449, 2016A1169, 2016B1492, 2017A1087, 2017B1464, 2018A1087, and 2018B1261).

Supplementary Materials

Supplementary 1. Figure S1: the flight speed of beetle with different loads. Figure S2: stimulation waveform and electrical current flow through the subalar muscle. Figure S3: EMG of nearby muscles during the electrical stimulation of the subalar muscle.

Supplementary 2. Movie S1: the response of the beetle due to electrical stimulation of subalar muscle.

References

- [1] R. S. Fearing, K. H. Chiang, M. H. Dickinson, D. L. Pick, M. Sitti, and J. Yan, "Wing transmission for a micromechanical flying insect," in *Proceedings 2000 ICRA. Millennium Conference. IEEE International Conference on Robotics and Automation. Symposia Proceedings (Cat. No. 00CH37065) (IEEE, 2000)*, vol. 2, pp. 1509–1516, San Francisco, CA, USA, 2000.
- [2] N. T. Jafferis, E. F. Helbling, M. Karpelson, and R. J. Wood, "Untethered flight of an insect-sized flapping-wing microscale aerial vehicle," *Nature*, vol. 570, no. 7762, pp. 491–495, 2019.
- [3] R. J. Wood, "The first takeoff of a biologically inspired at-scale robotic insect," *IEEE Transactions on Robotics*, vol. 24, no. 2, pp. 341–347, 2008.
- [4] H. V. Phan and H. C. Park, "Mimicking nature's flyers: a review of insect-inspired flying robots," *Current Opinion in Insect Science*, vol. 42, pp. 70–75, 2020.
- [5] H. V. Phan and H. C. Park, "Mechanisms of collision recovery in flying beetles and flapping-wing robots," *Science*, vol. 370, no. 6521, pp. 1214–1219, 2020.
- [6] G. C. H. E. de Croon, K. M. E. de Clercq, R. Ruijsink, B. Remes, and C. de Wagter, "Design, aerodynamics, and vision-based control of the DelFly," *International Journal of Micro Air Vehicles*, vol. 1, no. 2, pp. 71–97, 2009.
- [7] Y. Chen, H. Zhao, J. Mao et al., "Controlled flight of a micro-robot powered by soft artificial muscles," *Nature*, vol. 575, no. 7782, pp. 324–329, 2019.
- [8] K. Y. Ma, P. Chirarattananon, S. B. Fuller, and R. J. Wood, "Controlled flight of a biologically inspired, insect-scale robot," *Science*, vol. 340, no. 6132, pp. 603–607, 2013.
- [9] Y. Chen, H. Wang, E. F. Helbling et al., "A biologically inspired, flapping-wing, hybrid aerial-aquatic microrobot," *Science Robotics*, vol. 2, no. 11, 2017.
- [10] R. S. Fearing, S. Avadhanula, D. Campolo, M. Sitti, J. Yan, and R. Wood, "A micromechanical flying insect thorax," in *Neurotechnology for Biomimetic Robots*, D. R. Ayers, Ed., pp. 469–480, MIT Press, Cambridge, MA, USA, 2000.
- [11] M. A. Estrada, S. Mintchev, D. L. Christensen, M. R. Cutkosky, and D. Floreano, "Forceful manipulation with micro air vehicles," *Science Robotics*, vol. 3, no. 23, 2018.
- [12] S. B. Fuller, "Four wings: an insect-sized aerial robot with steering ability and payload capacity for autonomy," *IEEE Robotics and Automation Letters*, vol. 4, no. 2, pp. 570–577, 2019.
- [13] R. J. Wood, "Liftoff of a 60mg flapping-wing MAV," in *2007 IEEE/RSJ International Conference on Intelligent Robots and Systems*, pp. 1889–1894, San Diego, CA, USA, 2007.
- [14] Y. Zou, W. Zhang, and Z. Zhang, "Liftoff of an electromagnetically driven insect-inspired flapping-wing robot," *IEEE Transactions on Robotics*, vol. 32, no. 5, pp. 1285–1289, 2016.
- [15] M. Karásek, F. T. Muijres, C. D. Wagter, B. D. W. Remes, and G. C. H. E. de Croon, "A tailless aerial robotic flapper reveals that flies use torque coupling in rapid banked turns," *Science*, vol. 361, no. 6407, pp. 1089–1094, 2018.
- [16] G.-Z. Yang, J. Bellingham, P. E. Dupont et al., "The grand challenges of *Science Robotics*," *Science Robotics*, vol. 3, no. 14, 2018.
- [17] M. H. Dickinson, F. O. Lehmann, and K. G. Götz, "The active control of wing rotation by *Drosophila*," *The Journal of Experimental Biology*, vol. 182, no. 1, pp. 173–189, 1993.
- [18] R. F. Chapman, S. J. Simpson, and A. E. Douglas, *The Insects: Structure and Function*, Cambridge University Press, Cambridge, UK, 5th edition, 2012.
- [19] P. J. Gullan and P. S. Cranston, *The Insects: An Outline of Entomology*, Wiley-Blackwell, West Sussex, UK, 4th edition, 2010.
- [20] H. Straus-Duckheim, *Considérations générales sur l'anatomie comparée des animaux articulés, auxquelles on a joint l'anatomie descriptive du *Melolontha vulgaris* (hanneton)*, F.-G. Levrault, Ed., vol. 1, Levrault, Paris, 1828.

- [21] F. T. Muijres, M. J. Elzinga, J. M. Melis, and M. H. Dickinson, "Flies evade looming targets by executing rapid visually directed banked turns," *Science*, vol. 344, no. 6180, pp. 172–177, 2014.
- [22] M. H. Dickinson, C. T. Farley, R. J. Full, M. A. R. Koehl, R. Kram, and S. Lehman, "How animals move: an integrative view," *Science*, vol. 288, no. 5463, pp. 100–106, 2000.
- [23] A. D. Straw, S. Lee, and M. H. Dickinson, "Visual control of altitude in flying *Drosophila*," *Current Biology*, vol. 20, no. 17, pp. 1550–1556, 2010.
- [24] J. W. S. Pringle, *Insect Flight*, Cambridge University Press, Cambridge, UK, 1957.
- [25] H. Sato, T. T. Vo-Doan, S. Kolev et al., "Deciphering the role of a coleopteran steering muscle via free flight stimulation," *Current Biology*, vol. 25, no. 6, pp. 798–803, 2015.
- [26] H. Sato and M. M. Maharbiz, "Recent developments in the remote radio control of insect flight," *Frontiers in Neuroscience*, vol. 4, 2010.
- [27] H. Sato, C. W. Berry, Y. Peeri et al., "Remote radio control of insect flight," *Frontiers in Integrative Neuroscience*, vol. 3, p. 24, 2009.
- [28] Y. Li, J. Wu, and H. Sato, "Feedback control-based navigation of a flying insect-machine hybrid robot," *Soft Robotics*, vol. 5, no. 4, pp. 365–374, 2018.
- [29] A. J. Hinterwirth, B. Medina, J. Lockey et al., "Wireless stimulation of antennal muscles in freely flying hawkmoths leads to flight path changes," *PLoS One*, vol. 7, no. 12, 2012.
- [30] F. Cao, C. Zhang, T. T. Vo-Doan et al., "A biological micro actuator: graded and closed-loop control of insect leg motion by electrical stimulation of muscles," *PLoS One*, vol. 9, no. 8, 2014.
- [31] F. Cao and H. Sato, "Insect-computer hybrid robot achieves a walking gait rarely seen in nature by replacing the anisotropic natural leg spines with isotropic artificial leg spines," *IEEE Transactions on Robotics*, vol. 35, no. 4, pp. 1034–1038, 2019.
- [32] T. T. Vo-Doan, M. Y. W. Tan, X. H. Bui, and H. Sato, "An ultralightweight and living legged robot," *Soft Robotics*, vol. 5, pp. 17–23, 2018.
- [33] H. D. Nguyen, P. Z. Tan, H. Sato, and T. T. Vo-Doan, "Side-ways walking control of a cyborg beetle," *IEEE Transactions on Medical Robotics and Bionics*, vol. 2, no. 3, pp. 331–337, 2020.
- [34] R. Holzer and I. Shimoyama, "Locomotion control of a bio-robotic system via electric stimulation," in *Proceedings of the 1997 IEEE/RSJ International Conference on Intelligent Robot and Systems. Innovative Robotics for Real-World Applications. IROS'97*, vol. 3, pp. 1514–1519, Grenoble, France, 1997.
- [35] E. Whitmire, T. Latif, and A. Bozkurt, "Kinect-based system for automated control of terrestrial insect biobots," in *2013 35th Annual International Conference of the IEEE Engineering in Medicine and Biology Society (EMBC)*, pp. 1470–1473, Osaka, Japan, 2013.
- [36] C. J. Sanchez, C.-W. Chiu, Y. Zhou, J. M. González, S. B. Vinson, and H. Liang, "Locomotion control of hybrid cockroach robots," *Journal of The Royal Society Interface*, vol. 12, no. 105, p. 20141363, 2015.
- [37] H. Y. Choo, Y. Li, F. Cao, and H. Sato, "Electrical stimulation of coleopteran muscle for initiating flight," *PLoS One*, vol. 11, no. 4, 2016.
- [38] A. Bozkurt, R. F. Gilmour, A. Sinha, D. Stern, and A. Lal, "Insect-machine interface based neurocybernetics," *IEEE Transactions on Biomedical Engineering*, vol. 56, no. 6, pp. 1727–1733, 2009.
- [39] W. M. Tsang, A. L. Stone, Z. N. Aldworth et al., "Flexible splitting electrode for insect flight biasing using multisite neural stimulation," *IEEE Transactions on Biomedical Engineering*, vol. 57, no. 7, pp. 1757–1764, 2010.
- [40] A. Bozkurt, R. F. Gilmour, and A. Lal, "Balloon-assisted flight of radio-controlled insect biobots," *IEEE Transactions on Biomedical Engineering*, vol. 56, no. 9, pp. 2304–2307, 2009.
- [41] Y. Li, H. Sato, and B. Li, "Feedback altitude control of a flying insect-computer hybrid robot," *IEEE Transactions on Robotics*, vol. 37, 2021.
- [42] M. H. Dickinson, F.-O. Lehmann, and S. P. Sane, "Wing rotation and the aerodynamic basis of insect flight," *Science*, vol. 284, no. 5422, pp. 1954–1960, 1999.
- [43] S. C. Whitehead, T. Beatus, L. Canale, and I. Cohen, "Pitch perfect: how fruit flies control their body pitch angle," *Journal of Experimental Biology*, vol. 218, Part 21, pp. 3508–3519, 2015.
- [44] M. H. Dickinson and F. T. Muijres, "The aerodynamics and control of free flight manoeuvres in *Drosophila*," *Philosophical Transactions of the Royal Society B: Biological Sciences*, vol. 371, no. 1704, 2016.
- [45] V. Medici and S. N. Fry, "Embodied linearity of speed control in *Drosophila melanogaster*," *Journal of The Royal Society Interface*, vol. 9, no. 77, pp. 3260–3267, 2012.
- [46] F. T. Muijres, M. J. Elzinga, N. A. Iwasaki, and M. H. Dickinson, "Body saccades of *Drosophila* consist of stereotyped banked turns," *Journal of Experimental Biology*, vol. 218, no. 6, pp. 864–875, 2015.
- [47] S. N. Fry, N. Rohrseitz, A. D. Straw, and M. H. Dickinson, "Visual control of flight speed in *Drosophila melanogaster*," *Journal of Experimental Biology*, vol. 212, no. 8, pp. 1120–1130, 2009.
- [48] S. Vogel, "Flight in *Drosophila*," *Journal of Experimental Biology*, vol. 44, no. 3, pp. 567–578, 1966.
- [49] C. N. Balint and M. H. Dickinson, "The correlation between wing kinematics and steering muscle activity in the blowfly *Calliphora vicina*," *Journal of Experimental Biology*, vol. 204, no. 24, pp. 4213–4226, 2001.
- [50] A. E. Kammer, "The motor output during turning flight in a hawkmoth," *Manduca sexta. Journal of Insect Physiology*, vol. 17, no. 6, pp. 1073–1086, 1971.
- [51] D. Springthorpe, M. J. Fernández, and T. L. Hedrick, "Neuromuscular control of free-flight yaw turns in the hawkmoth *Manduca sexta*," *Journal of Experimental Biology*, vol. 215, no. 10, pp. 1766–1774, 2012.
- [52] C. N. Balint and M. H. Dickinson, "Neuromuscular control of aerodynamic forces and moments in the blowfly, *Calliphora vicina*," *Journal of Experimental Biology*, vol. 207, no. 22, pp. 3813–3838, 2004.
- [53] R. Elson and H.-J. Pflüger, "The activity of a steering muscle in flying locusts," *Journal of Experimental Biology*, vol. 120, no. 1, pp. 421–441, 1986.
- [54] J. R. Stowers, M. Hofbauer, R. Bastien et al., "Virtual reality for freely moving animals," *Nature Methods*, vol. 14, no. 10, pp. 995–1002, 2017.

- [55] W. Kutsch, "Transmission of muscle potentials during free flight of locusts," *Computers and Electronics in Agriculture*, vol. 35, no. 2-3, pp. 181–199, 2002.
- [56] H. Fischer, H. Kautz, and W. Kutsch, "A radiotelemetric 2-channel unit for transmission of muscle potentials during free flight of the desert locust, *Schistocerca gregaria*," *Journal of Neuroscience Method*, vol. 64, no. 1, pp. 39–45, 1996.
- [57] N. Ando and R. Kanzaki, "Changing motor patterns of the 3rd axillary muscle activities associated with longitudinal control in freely flying hawkmoths," *jzoo*, vol. 21, no. 2, pp. 123–130, 2004.
- [58] T. T. Vo-Doan and A. D. Straw, "Millisecond insect tracking system," <http://arxiv.org/abs/2002.12100>.
- [59] J. Sakakibara, J. Kita, and N. Osato, "Note: high-speed optical tracking of a flying insect," *The Review of Scientific Instruments*, vol. 83, no. 3, 2012.
- [60] M. Mischiati, H.-T. Lin, P. Herold, E. Imler, R. Olberg, and A. Leonardo, "Internal models direct dragonfly interception steering," *Nature*, vol. 517, no. 7534, pp. 333–338, 2015.